

# Improved Viewing Quality of 3-D Images in Computational Integral Imaging Reconstruction Based on Lenslet Array Model

Dong-Hak Shin, Byounggho Lee, and Eun-Soo Kim

*ABSTRACT*—In this letter, we propose a novel computational integral imaging reconstruction technique based on a lenslet array model. The proposed technique provides improvement of viewing images by extracting multiple pixels from elemental images according to ray tracing based on the lenslet array model. To show the feasibility of the proposed technique, we analyze it according to ray optics and present the experimental results.

*Keywords*—3-D display, integral imaging, computational reconstruction.

## I. Introduction

There are several methods to display a three-dimensional (3-D) object, for example, stereoscopy, holography, integral imaging (II) and so on [1]. Among them, II, which was first proposed by Lippmann in 1908, can record and reconstruct a 3-D object using a white light source [2]-[7]. It has full parallax, continuous viewing points, and observers experience no visual fatigue from stereoscopy. In the pickup process of II, direction and intensity information of the rays coming from a 3-D object are spatially sampled by use of a lenslet array (or pinhole array) and 2-D image sensor. The recorded images through each lenslet (or pinhole) have their own perspective and demagnified images of a 3-D object. These images are called

elemental images. A real image is reconstructed through the lenslet array when the elemental image is displayed on a 2-D display device.

Recently, there has been a great interest in computational integral imaging reconstruction (CIIR) [8]-[11]. These methods can be classified into plane-based CIIR techniques [8], [9] and view-based CIIR techniques [10], [11]. Plane-based CIIR generates 3-D images by changing the reconstructed image plane. In this case, the reconstructed 3-D images are different according to the position of the image plane. On the other hand, view-based CIIR generates 3-D images by extracting a single pixel from corresponding element images based on a pinhole array model. Here, the reconstructed 3-D images are different from each other according to the observation points. That is, view-based CIIR can show perspective in the lateral direction. However, it has the problem of low-viewing resolution because only a single pixel from the corresponding pinhole is extracted.

In this letter, to improve the viewing resolution of reconstructed 3-D images in CIIR, we propose a view-based CIIR technique based on a lenslet array model. The proposed technique can extract multiple pixels from each lenslet according to ray tracing based on the lenslet array model. The extraction of multiple pixels can be easily found in an optical display system using a large lenslet array [12], [13]. In this sense, the proposed scheme can be considered to mimic an II display system. To show the feasibility of the proposed technique, we analyze it according to ray optics and present the experimental results.

## II. View-Based CIIR Based on a Lenslet Array Model

Figure 1 shows the structure of view-based CIIR. The

Manuscript received Jan. 20, 2006; revised Mar. 27, 2006.

This research was supported by the Ministry of Education & Human Resources Development, Korea, under the University Specializing Realistic IT Research Center.

Dong-Hak Shin (phone: +82 2 940 5118, email: shindh2@daisy.kw.ac.kr) is with 3D Display Research Center, Kwangwoon University, Seoul, Korea.

Byounggho Lee (email: byounggho@snu.ac.kr) is with the School of Electrical Engineering, Seoul National University, Seoul, Korea.

Eun-Soo Kim (email: eskim@daisy.kw.ac.kr) is with the Department of Electronic Engineering, Kwangwoon University, Seoul, Korea.

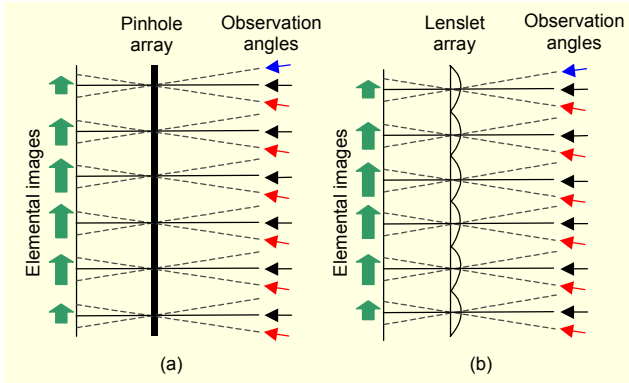


Fig. 1. View-based CIIR: (a) pinhole array model and (b) lenslet array model.

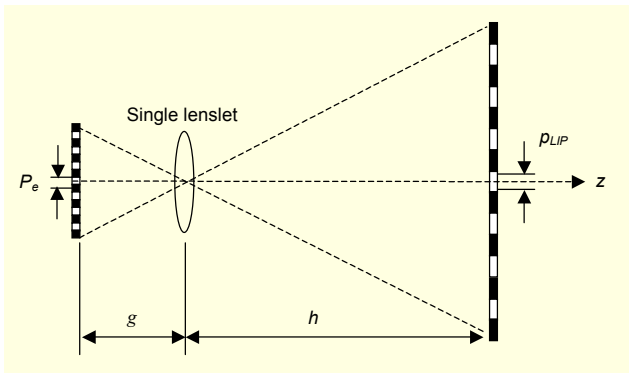


Fig. 2. Pixel mapping of single lenslet.

pinhole array is used in conventional techniques as shown in Fig. 1(a). Here, the elemental images are observed through the pinhole array from an arbitrary viewing angle. Then, we can observe a single pixel from a single pinhole. The resolution of reconstructed images is equal to the number of pinholes or elemental images. In general, we obtain low-resolution 3-D images in conventional CIIR because the number of elemental images is limited by the pickup device.

To improve the resolution of reconstructed 3-D images in view-based CIIR, we introduce a lenslet array model into a conventional technique as shown in Fig. 1(b). The proposed technique includes a lens characteristic based on a lenslet array model. We consider the effect of the distance between a lenslet array and an elemental image plane. Figure 2 depicts the scheme for defining the pixel mapping between an elemental image plane (EIP) and a lenslet image plane (LIP). We assume that the focal length of a single lenslet is  $f$ , the distance between the EIP and the single lenslet is  $g$ , and the distance between the single lenslet and the LIP is  $h=gf/(g-f)$ . If the pitch of the elemental image at the EIP is  $p_e$ , the pitch of the integrated image at the LIP becomes

$$p_{LIP} = \frac{h}{g} p_e. \quad (1)$$

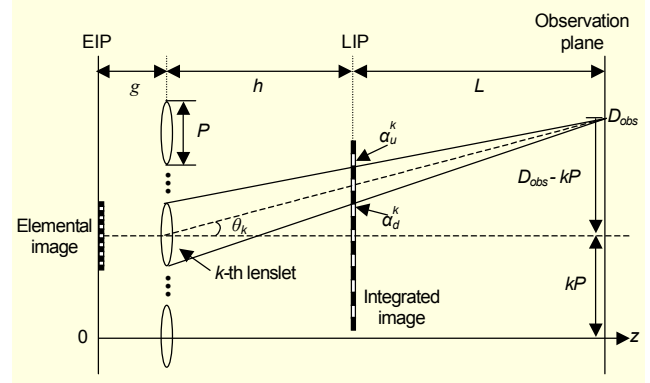


Fig. 3. Ray diagram for calculating the number of pixels observed.

This means that the elemental image is simply magnified at the LIP.

Figure 3 illustrates the scheme of the proposed technique according to ray optics at an observation point. Suppose that the lenslet array is composed of square  $M$  lenslets, and that an integrated image in the LIP is observed from an observation point,  $D_{obs}$ . Here, the distance between the observation point and the LIP is  $L$ . Rays coming from the  $k$ -th elemental image displayed on a display panel are reimaged as the integrated image in the LIP and then observed at  $D_{obs}$  as shown in Fig. 3. To explain our technique, we first calculate two parameters for the  $k$ -th lenslet; observation angle  $\theta_k$  and observation area  $D_k$ . As shown in Fig. 3, the observation angle through the optical axis of the  $k$ -th lenslet from  $D_{obs}$  can be simply calculated by

$$\theta_k = \tan^{-1} \left( \frac{D_{obs} - kP}{h + L} \right). \quad (2)$$

Here, integer  $k$  is 1 to  $M$ , and  $P$  is the pitch of the lenslet array. Next, we compute the observation area to be observed through the  $k$ -th lenslet from  $D_{obs}$ . Let us consider two lines from  $D_{obs}$  to two edges of the  $k$ -th lenslet and their intersection points at the LIP, which are denoted by

$$a_u^k = \left( \frac{h}{h + L} \right) D_{obs} + \left( \frac{L}{h + L} \right) \left( k + \frac{1}{2} \right) P \quad (3)$$

and

$$a_d^k = \left( \frac{h}{h + L} \right) D_{obs} + \left( \frac{L}{h + L} \right) \left( k - \frac{1}{2} \right) P. \quad (4)$$

Then, the range between these intersection points becomes our observation area  $D_k$ , which is represented by

$$D_k = a_u^k - a_d^k = \frac{PL}{h + L}. \quad (5)$$

Here,  $D_k$  becomes constant regardless of  $k$ .

The number of pixels extracted from an elemental image through the  $k$ -th lenslet becomes

$$N_k = \frac{D_k}{p_{LIP}} = \frac{PL}{(h+L)p_{LIP}}. \quad (6)$$

Equation (6) means that we can observe  $N_k$  pixels through the  $k$ -th lenslet when the 3-D image is seen. Finally, we can obtain  $\theta_k$  and  $N_k$  as given by (2) and (6). With them, we can simply extract  $N_k$  pixels at the pixel observed from the  $\theta_k$  angle for the  $k$ -th lenslet as shown in Fig. 4. First,  $\theta_k$  is calculated using (2). Next, the center pixel is chosen as the intersection point between elemental image and a ray incident at the  $\theta_k$  angle from the lenslet. Finally,  $N_k$  pixels are extracted at the center pixel. In order to form a full 3-D viewing image, we repeat this process for all  $k$  from 1 to  $M$ .

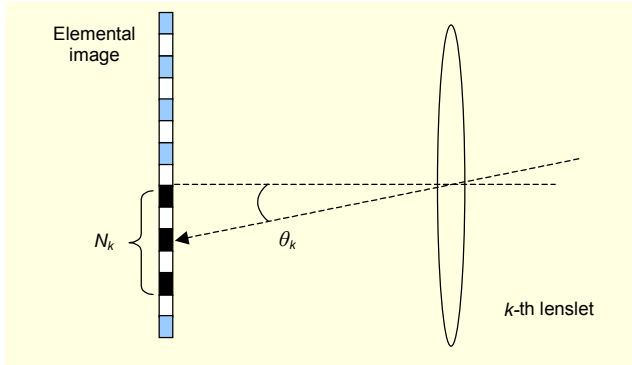


Fig. 4. Principle of multi-pixel extraction from single elemental image.

### III. Experiments and Results

To show the feasibility of the proposed technique, preliminary experiments were performed. The object is composed of a toy car and toy octopus, as shown in Fig. 5(a). The toy car and toy octopus are positioned at 3 cm and 10 cm from the lenslet array. The elemental images are captured by direct camera pickup, as shown in Fig. 5(b). The pickup lenslet array has  $49 \times 37$  lenslets. Each lenslet, whose focal length  $f$  is 3 mm, is square-shaped and has a uniform size  $p_e$  of  $1.08 \text{ mm} \times 1.08 \text{ mm}$ . Each elemental image has 30 pixels. We used  $g = 3.5 \text{ mm}$  and then  $h = 21 \text{ mm}$ . The observation plane is located at  $L = 2 \text{ m}$ .

For all  $k$  and various  $D_{obs}$ , we computed  $\theta_k$  and  $N_k$  according to (2) and (6). In a pickup condition, we obtained  $N_k = 5$  pixels for all  $k$ . We synthesized a full 3-D viewing image by extracting  $5 \times 5$  pixels from each elemental image for all the lenslets. Figure 6 shows the 3-D viewing images reconstructed computationally by use of the proposed technique. For

comparison, we also show the results of using a conventional CIIR technique [10] in which we can observe only a single pixel from a single pinhole as shown in Fig. 1(a). From Fig. 6, we see that the resolution of a viewing image by use of the proposed technique is 25 times higher than that of the conventional technique. Figure 7 presents the reconstructed 3-D images according to various observation angles. We can observe different reconstruction images according to the observation angles.

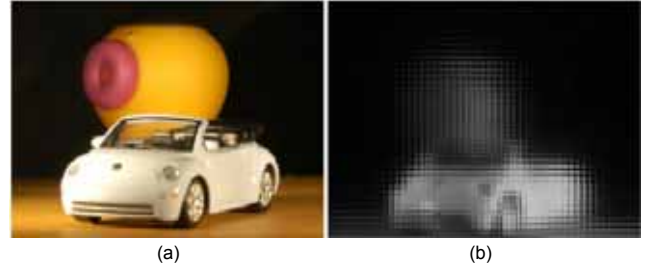


Fig. 5. (a) 3-D objects and (b) recorded elemental images.



Fig. 6. 3-D viewing image observed: (a) conventional and (b) proposed methods.

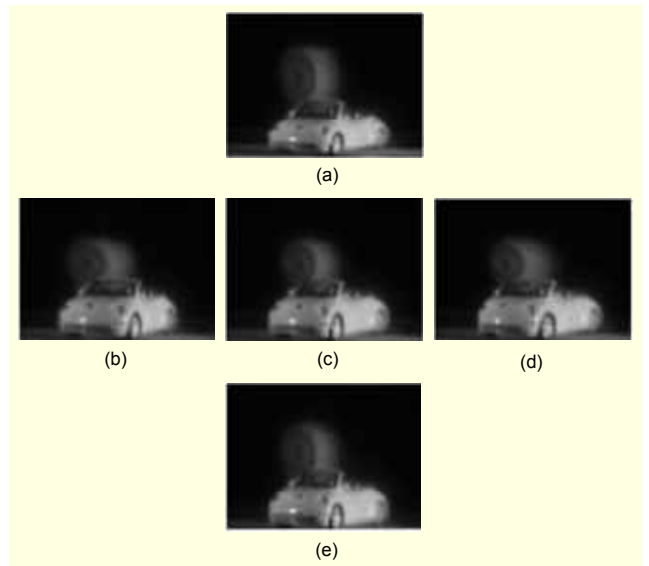


Fig. 7. 3-D viewing images according to various observation positions: (a) top view, (b) left view, (c) front view, (d) right view, and (e) bottom view.

## IV. Conclusion

In conclusion, we proposed a computational reconstruction technique in which a 3-D image is reconstructed by extracting multiple pixels from each elemental image in computational II. The proposed technique can improve the viewing resolution of a reconstructed 3-D image.

Even though the proposed technique was demonstrated successfully, more improvement of reconstructed images is required. To achieve this, we need more elemental images. Many elemental images can be obtained optically or computationally [5], [14]-[16].

## References

- [1] S. A. Benton, *Selected Papers on Three-Dimensional Displays*, SPIE Optical Engineering Press, Bellingham, WA, 2001.
- [2] G. Lippmann, "La Photographie Integrale," *Comptes-Rendus Academie des Sciences*, vol. 146, 1908, pp. 446-451.
- [3] F. Okano, H. Hoshino, J. Arai, and I. Yuyama, "Real-Time Pickup Method for a Three-Dimensional Image Based on Integral Photography," *Appl. Opt.*, vol. 36, 1997, pp. 1598-1603.
- [4] S.-W. Min, B. Javidi, and B. Lee, "Enhanced Three-Dimensional Integral Imaging System by Use of Double Display Devices," *Appl. Opt.*, vol. 42, 2003, pp. 4186-4195.
- [5] J.-S. Jang and B. Javidi, "Improved Viewing Resolution of Three-Dimensional Integral Imaging with Nonstationary Micro-Optics," *Opt. Lett.*, vol. 27, 2002, pp. 324-326.
- [6] S.-H. Hong, J.-S. Jang, and B. Javidi, "Three-Dimensional Volumetric Object Reconstruction Using Computational Integral Imaging," *Opt. Express*, vol. 12, 2004, pp. 483-491.
- [7] D.-H. Shin, M. Cho, and E.-S. Kim, "Computational Implementation of Asymmetric Integral Imaging by Use of Two Crossed Lenticular Sheets," *ETRI J.*, vol. 27, 2005, pp. 289-293.
- [8] S. Hong, J.-S. Jang, and B. Javidi, "Three-Dimensional Volumetric Object Reconstruction Using Computational Integral Imaging," *Opt. Express*, vol. 12, 2004, pp. 483-491.
- [9] D.-H. Shin, M. Cho, K.-C. Park, and E.-S. Kim, "Computational Technique of Volumetric Object Reconstruction in Integral Imaging by Use of Real and Virtual Image Fields," *ETRI J.*, vol. 27, 2005, pp. 708-712.
- [10] H. Arimoto and B. Javidi, "Integral Three-Dimensional Imaging with Digital Reconstruction," *Opt. Lett.* vol. 26, 2001, pp. 157-159.
- [11] T. Naemura, T. Yoshida, and H. Harashima, "3-D Computer Graphics Based on Integral Photography," *Opt. Express*, vol. 8, 2001, pp. 255-262.
- [12] J.-H. Park, S. Jung, H. Choi, and B. Lee, "Integral Imaging with Multiple Image Planes Using a Uniaxial Crystal Plate," *Opt. Express*, vol. 11, 2003, pp. 1862-1875.
- [13] Y. Kim, J.-H. Park, H. Choi, S. Jung, S.-W. Min, and B. Lee, "Viewing-Angle-Enhanced Integral Imaging System Using a Curved Lens Array," *Opt. Express*, vol. 12, 2004, pp. 421-429.
- [14] A. Stern and B. Javidi, "Shannon Number and Information Capacity of Integral Images," *J. Opt. Soc. Am. A.*, vol. 21, 2004, pp. 1602-1612.
- [15] A. Stern and B. Javidi, "Three-Dimensional Image Sensing and Reconstruction with Time-Division Multiplexed Computational Integral Imaging," *Appl. Opt.*, vol. 42, 2003, pp. 7036-7042.
- [16] D.-C. Hwang, J.-S. Park, S.-C. Kim, D.-H. Shin, and E.-S. Kim, "Magnification of 3-D Reconstructed Images in Integral Imaging Using Intermediate-View Reconstruction Technique," *Applied Optics*, vol. 45, no. 19, 2006, pp. 4631-4637.